ANEXA 1.A

Call: 2024 **Project acronym: CEHDEP**

FAIR Research Programme / Experiment: CBM

Annual Summary Document*

Year: 2024

Months: 6

Project Title:

CBM experiment on the horizon - detectors, electronics, data acquisition and physics/CEHDEP

Project Work Plan (according to the contract)

Stage: I. *Contribution of DFH in 2024, through research and development activities, on the way towards the materialization of the CBM experiment at FAIR.*

Activities:

A versatile architecture of MSMGRPC with direct gas flow through gas gaps will be designed, components fabricated and prototypes assembled; the gas distribution system for equilibrated direct flow and the experimental configuration for functionality tests will be made. Aging effects investigations using high flux X-ray tubes as well as extensive in-house tests of the MSMGRPC performance using cosmic rays will be done. Optimization studies of the TRD-2D entrance window to enhance the transmission of soft transition radiation photons according to the radiator design proposed for the TRD-CBM setup will be done. The design and construction of the TRD-2D production readiness prototype will be done. A special emphasize will be put on anode wire alignment, gas tightness and gain uniformity. The design of a versatile motherboard for testing large amount of encapsulated FASP CHIPs from production engineering will be done. The design and realization of a mechanical device for control and quality assurance in the assembly process of the TRD-2D detector will be made.

* Please fill in all the required items and do not alter the template

1. Cover Page (max 1 pag)

- Specify scientific focus of the group and role in the collaboration
  Contribution of DFH in 2024, through research and development activities, on the way towards the materialization of the CBM experiment at FAIR.

- Summary of accomplishments during the reporting period

CBM-TOF: assembling and successful testing of direct flow prototypes with different granularities for different polar angle regions of the CBM-ToF inner zone. The direct flow prototypes demontrated the possibility of mitigation of the aging effect in multistrip, multigap resistive plate chambers through a faster removal of the chemical compunds resulted from exposure to radiation together with the minimization of the active area in contact with the spacers.

Studies of the structure and materials used in the construction of the TRD2D entrance window. These studies are aimed to enhance the transmission of soft Transition Radiation (TR) photons and therefore to increase the separation of electrons (generating these TR photons) from the background.

A full-production TRD2D prototype together with all the technological steps towards its completion is of mandatory importance, for starting the construction of the 40 TRD2D chambers, which have to be installed for first data taking in 2028. The design, construction and in-house tests of these prototypes have been thoroughly investigated.

2. Scientific accomplishments

- Results obtained during the reporting period

2.1. CBM - TOF:

Design and construction of a versatile architecture of MSMGRPC with direct gas flow through the gas gaps.

Due to the high interaction rates at which the CBM experiment is designed to run, the chambers of the CBM-TOF wall have to cope with anticipated counting rates ranging between 0.1 kHz/cm^2 up to a few tens of kHz/cm^2, depending on their location [1, 2]. In view of their use over the lifetime of the experiment, especially in the challenging counting rates mentioned above, comprehensive aging investigations are mandatory. On a long term operation, the aging effects are reflected in an increase of the dark current and dark counting rate which might impact the chamber performance and also could lead to an artificial increase of the data volume in a free-running readout mode.

Detailed aging investigations were performed [3] using the high activity (360 kCi) ^{60}Co source [4] of IFIN-HH. A gas pollution effect was evidenced by the chemical composition of the layers deposited on both surfaces of the resistive electrodes of a MSMGRPC prototype with classical gas exchange via diffusion. Moreover, enhanced depositions and larger noise rates were observed around the nylon spacers (fishing line) which define the gas gaps between resistive electrodes. With the aim to reduce the observed aging effects, we focused our efforts to a faster removal from the gas gaps of the chemical compounds produced during irradiation, preventing their depositions on the glass surfaces. We have developed MSMGRPC prototypes with a direct gas flow architecture and minimization of the number of spacers in the active area. The constructive details of the first prototypes with a direct gas flow through the gaps between the resistive electrodes and

the highest granularity of the CBM-TOF wall (MRPC1a, 56 mm strip length), together with their in-beam tests are comprehensively described in [5].

Detailed aging investigations using a high X-ray flux showed better behaviour of the direct flow prototype in comparison with a prototype with classical gas exchange via diffusion in terms of the dark current and dark counting rate [6].

In the current design, the CBM-TOF inner wall is equipped with a total number of 316 Multi-Strip Multi-Gap Resistive Plate Chambers (MSMGRPCs). As a function of polar angle, different regions of granularity are covered by three types of chambers, differentiated only by their strip length (MRPC1a of 56 mm, MRPC1b of 96 mm and MRPC1c of 196 mm) while the strip pitch (9.02 mm) and the inner architecture are the same.
Three types of MSMGRPCs prototypes (corresponding to MRPC1a, MRPC1b and MRPC1c types) with direct gas flow and minimization of the spacers in contact with the active area of the chamber (the outermost fishing line spacers are positioned outside the active area) were assembled and tested in the laboratory of HPD/IFIN-HH.
In a first step, the prototypes were investigated for the aging effects. Two mini X-ray tubes were aligned next to each other and positioned in front of the housing box, at a certain distance (see Fig.1) which assured an almost uniform exposure of the chamber to the high X-ray flux. The 32 strips of each MSMGRPC prototype were readout at both ends by eight front-end electronics cards based on NINO ASIC. Each card provides besides the information of the time of the rising and falling edge for each of its eight channels, a common logic OR signal. The logic AND between the OR signals of the two ends of each group of eight strips was fed into the input of a scaler, recording the rate of the signals. The average counting rate per unit area of the chamber was obtained as the arithmetic mean of the recorded rates divided by the corresponding strip area.

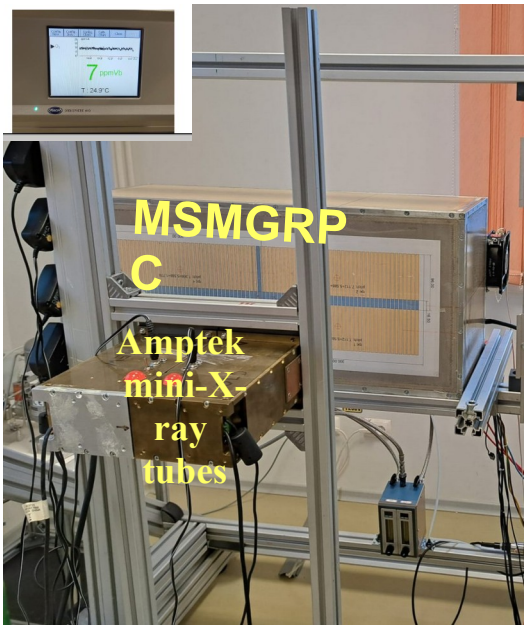

Fig. 1 Experimental setup for X-ray aging tests.

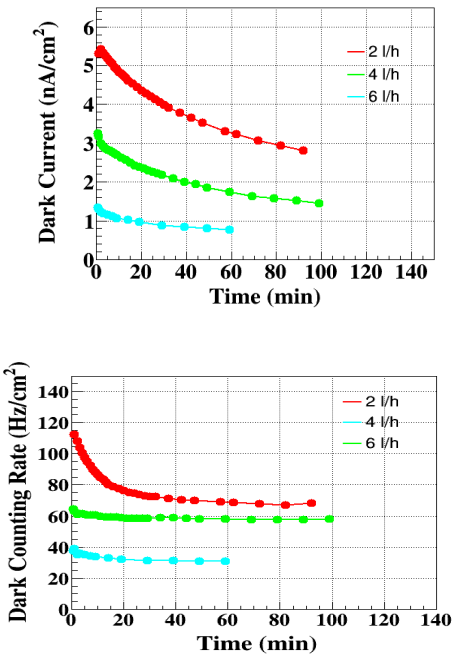

Fig.2 Dark current (top) and dark counting rate (bottom) at different gas flow rates.

We exposed the chambers at the highest counting rate obtained with two X-ray tubes, of 28 kHz/cm^2, for about 7 hours and monitored the current and counting rate. After this time interval we recorded the dark current and dark rate behaviour over about 2 hours. We observed the improvement brought by a higher gas flow, as it is shown in Fig.2 , which also demonstrates that we face a gas pollution effect and not a glass aging effect.

Cosmic ray tests

After the aging tests, the performance of the chambers in terms of efficiency and time resolution was tested using cosmic rays. We stacked all tree chambers, closed them in the housing box and flushed each one with an equal gas flow rate of 2 l/h, provided by a special system of flow regulators. MRPC1a and MRPC1c chambers sandwiched between them the MRPC1b prototype, as it is shown in Fig.3. The housing box was also flushed with the working gas mixture in order to preserve the gas purity inside the chambers.

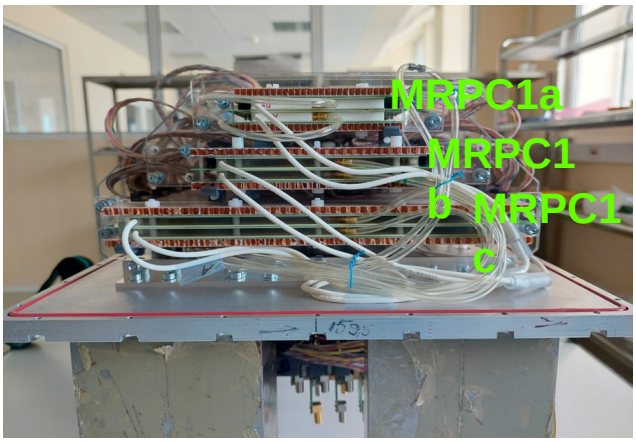

Fig.3 Stacked chambers for cosmic ray test.

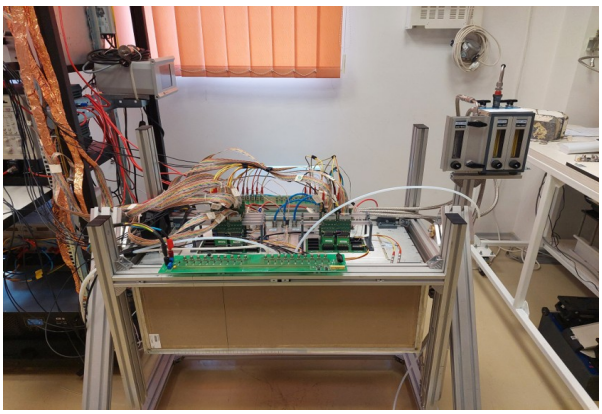

Fig.4 Experimental setup for cosmic ray test.

For each chamber, 16 strips were readout at both ends by NINO [7] based FEE. The LVDS signals delivered by the FEE were fed into the inputs of CAEN V1290A TDCs.

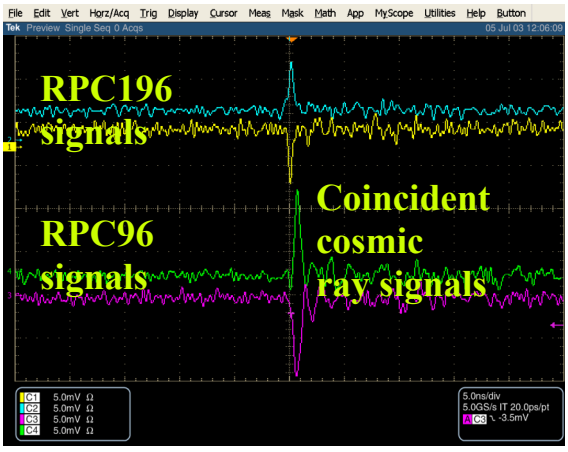

Fig.5 Cincident cosmic signals in two MSMGRPCs.

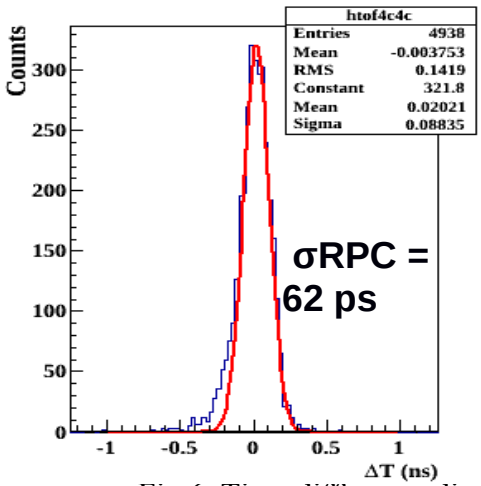

Fig.6 Time difference distribution.

The DAQ system was triggered by the coincident signal between MRPC1a and MRPC1c chambers.

The measured efficiency for the MRPC1b chamber, defined as the number of coincident signals in all three chambers divided by the number of coincident signals in MRPC1a and MRPC1c was of 95% for 2 x 6 kV applied high voltage. The time difference distribution between MRPC1b and MRPC1a, corrected for the slewing effect, is shown in Fig. 6. A single counter time resolution of 62±2 ps was obtained from the Gauss fit of the time difference spectrum, supposing equal contributions of both chambers. The measured efficiency for the MRPC1b chamber, defined as the number of coincident signals in all three chambers divided by the number of coincident signals in MRPC1a and MRPC1c was of 95% for 2 x 6 kV applied high voltage. The time difference distribution between MRPC1b and MRPC1a, corrected for the slewing effect, is shown in Fig. 6. A single counter time resolution of 62±2 ps was obtained from the Gauss fit of the time difference spectrum, supposing equal contributions of both chambers.

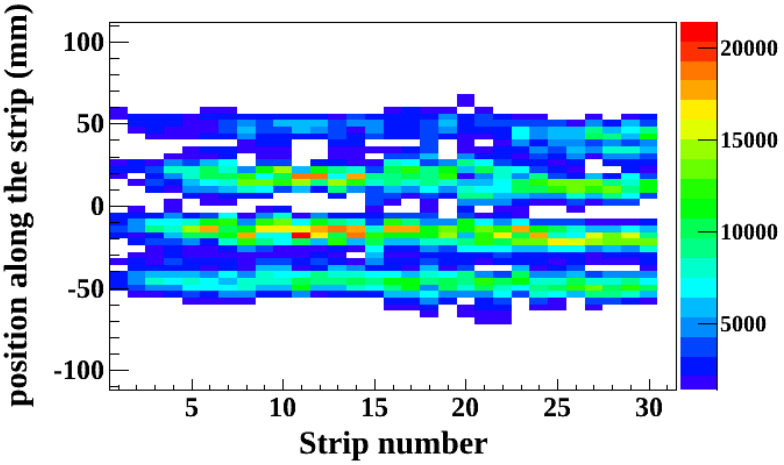

Fig.7 Position along the strip versus strip number.

A mapping of the active area of the chambers in a self trigger mode operation of the DAQ system revealed still an activity around the spacer positions. This can be seen in the two-dimensional representation of the position along the strip versus strip number shown in Fig.7-left.

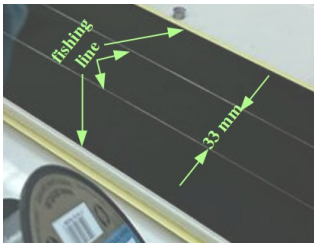

Fig.8 Glass plate with fishing lines

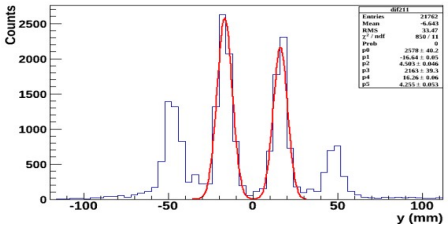

Fig.9 Position along one strip.

The position along the strip was obtained based on the time difference between the times measured at two ends of each strip.

Knowing the distance between the fourth nylon line spacers stretched across the strips of the MRPC1b prototype, as it si shown in Fig.8, a calibration in position was possible. From the Gauss fit of the two middle peaks seen in the one dimensional projection along one strip (Fig.9), an accuracy of the position determination along the strip of 4.5±0.05 mm was estimated. Based on the distance between the two middle peaks and the TDC calibration of 25 ps/bin, a 17 cm/ns signal velocity propagation along the strip was determined.

The mapping in self triggered mode for the MRPC1c prototype evidenced a similar structure with a higher activity around the spacers. Similar results in terms of accuracy of the position determination (4.9±0.05 mm) and signal propagation velocity (16.5 cm/ns) were obtained. Although a significant improvement was obtained with the direct flow architecture and minimization of the active area in contact with the continuous nylon line spacers, the presented results of the cosmic tests performed on aged chambers show that there is still room for improvements.

In order to minimize further the aging effects around the spacers, we are going to replace the continuous nylon fishing line by discrete pad spacers made of polyimide. In a next step we will perform comparatively aging investigations for chambers based on such discrete spacers relative to these ones based on continous nylon spacers.

References:

1. CBM Collaboration, N. Herrmann ed., CBM-TOF TDR, October 2014.
2. I. Deppner et al., The CBM time-of-flight system, J. Instrum., 14 (2019) C09020.
3. D. Bartos et al., Ageing studies of multi-strip multi-gap resistive plate counters based on low resistivity glass electrodes in high irradiation dose, Nucl. Instrum. Meth. A 1024 (2022) 166122.
4. IRASM center/IFIN-HH, Bucharest. URL https://www.nipne.ro/IRASM.php
5. M. Petris et al., High time resolution, two-dimensional position sensitive MSMGRPC for high energy experiments, Nucl. Instrum. Meth. A , 1045(2023) 167621.
6. V. Aprodu et al., Aging suppression, high time resolution and 2d-position sensitive multi-strip multi-gap resistive plate counter for high rate experiments, Nucl. Instrum. Meth. A , 1049 (2023) 168098
7. F. Anghinolfi et al., NINO: An ultra-fast and low-power front-end amplifier/discriminator ASIC designed for the multigap resistive plate chamber, Nucl. Instrum. Meth. A , 533 (2004) 183

2.2 CBM TRD-2D

Before starting the assembling of CBM TRD-2D chambers, we have done some absorption studies of different entrance window configurations in order to decrease as much as possible the absorption of low energy TRs, still maintaining at a reasonable level the mechanical deformation at a ~ 1 mbar pressure difference.

A few samples of different configurations for the entrance window were assembled and measured. An overview of such samples and their structure is presented in Fig. 1. The results of these measurements are presented in Fig.3. As could be seen, a structure based on 135 μm carbon fiber foil + 25 μm Al aluminised Mylar + 9 mm honeycomb + 20μm aluminsed kapton foil, has an absorption of 31 %, to times lower than the absorption of sample 2, used as entrance window of the prototypes mentioned above and more than 2 times less than the ALICE-TRD entrance window (sample 9). For such a configuration, the measured mechanical deformation in the middle of the window of 60x60 cm^2, the size used for the TRD chambers in the inner zone of the CBM-TRD sub-detector, is of ~ 1.75 mm at 1 mbar pressure difference.

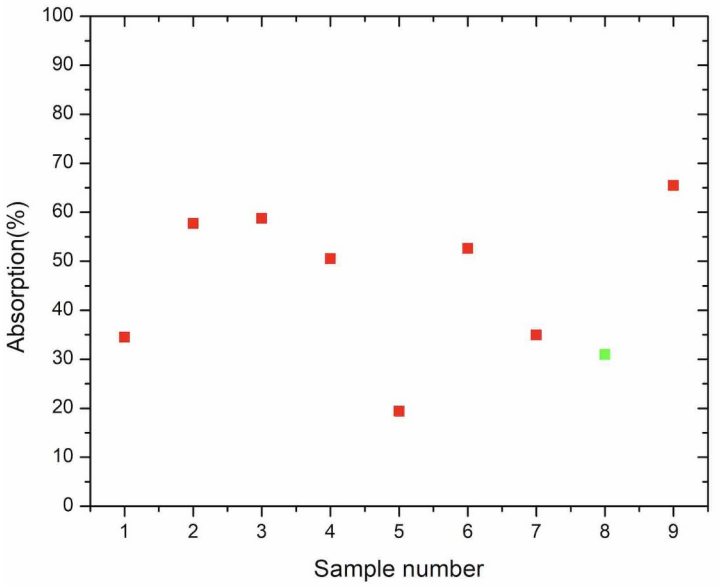

Fig. 2: Absorption value for 5.9 keV ^{55}Fe X rays for the samples presented in Fig.1.

The TRD2D read-out chamber has to fulfill the mutually exclusive requirements of lightness and mechanical rigidity, coupled with sub-millimeter precision of relative internal alignment of the components. The first element under scrutiny was the realization of anode and cathode electrodes. The anodes are used in the TRD2D design not only to generate charge amplification but also to

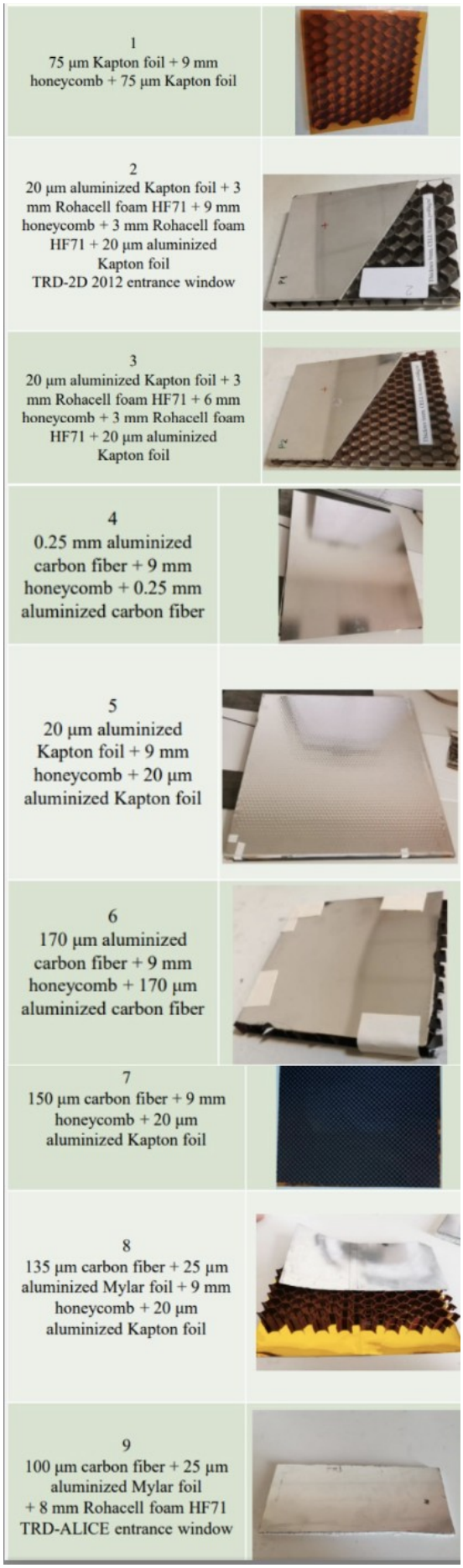

Fig. 1: The structure of different samples used in the absorption measurement

provide position sensitive information. As such they imply a strict requirement for a micrometer precision alignment wrt. the chamber and a well controlled mechanical tension during installation. In Fig. 3 an image under microscope is used to prove the positioning of various constructive elements of the TRD2D chamber. In figure, two opposite corners of the chamber are shown aligned on the picture wrt. the alignment holes (dashed yellow). The anode wires are emphasized in yellow while cathodes in red. The projection from the left corner to the next, and the observed difference from the ctual positioning of the component illustrate the level of alignment obtained during construction.

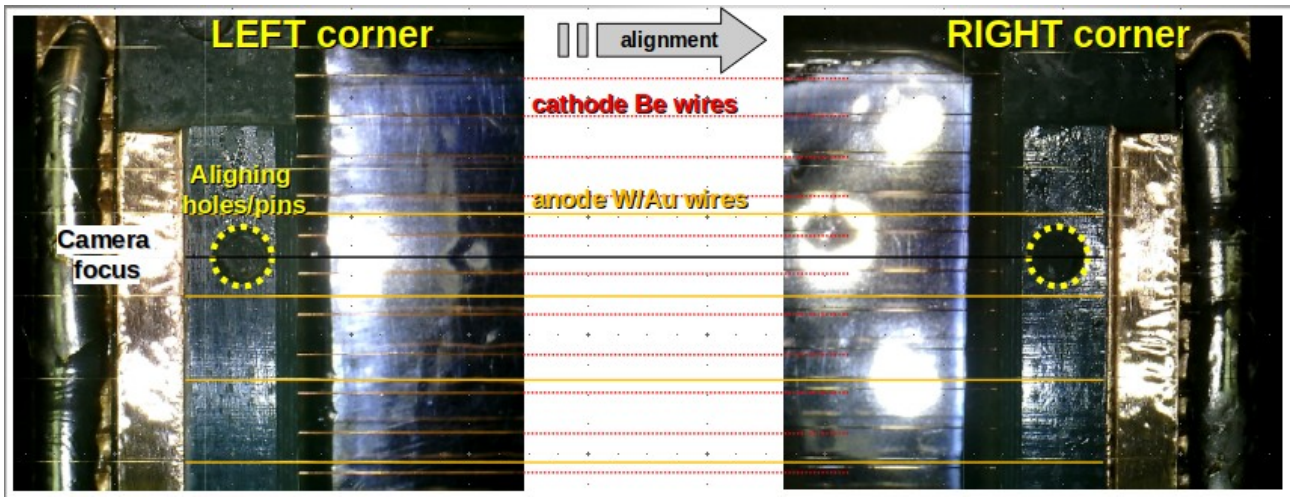

Fig. 3: Alignment of constructive details from the chamber design with anode and cathode wires, for two opposite corners of the TRD2D prototype. Image magnified under microscope used for alignment.

The mechanical tension on the wire electrodes is important as we have assure stable electric fields during operation. After positioning and gluing the anode wires in place a dedicated tool is used to check that the 0.5 N used to pre-tension the wires was kept during installation procedure. In Fig. the post installation measurement on the mechanical tension of each individual anode wire is presented. The target value is marked in yellow while the mean of the measured points in red. Points marked in red represent wires which have deviations larger than 10 % wrt. the mean value and are marked as "probable bad". The real threshold value for the acceptance tests will be defined by estimating the gain uniformity in the next paragraph.

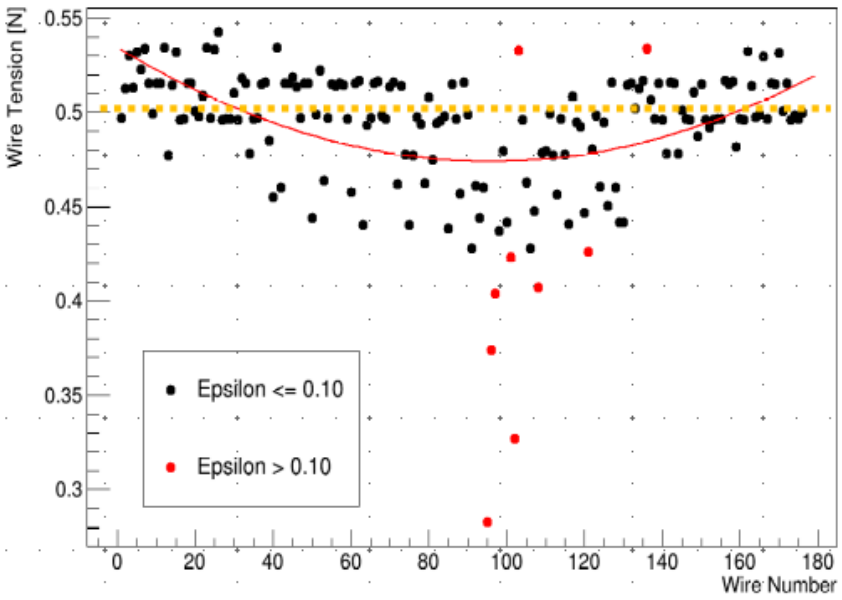

Fig. 4: Anode wire tension after gluing on the chamber support with cathode plane installed.

A fine scan of the chamber was performed in order to determine its gain function. The scan was performed by illuminating the chamber with a ^{55}Fe source in a collimated setup. The source was moved by 1 mm with a step-by-step CNC in front of the detector, perpendicular to the anode wire direction. Each time the current measured on the full anode electrode was registered for 7 s. The correlation of I_{anode} (nA) as function of the position on the detector is shown in Fig. 5, for two positions wrt. the detector, across its middle region (red) and close to the edge where the electrode is glued (blue). Both measurements show qualitatively the same components:

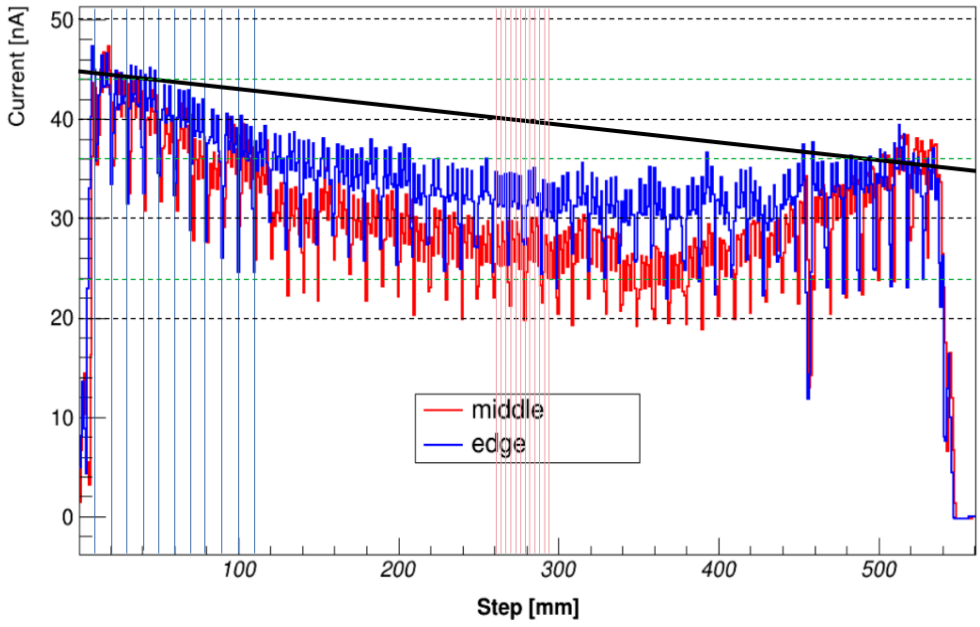

F

ig. 5: Correlation of anode wire current with the position on the detector for two measurements done perpendicular to the anode wire direction.

1. A general *linear decreasing trend* of 8 nA (~ 20 %) from left to right correlated with a lack of parallelism between the pad-plane and the anode electrode;
2. A *general parabolic dependence* over the whole scanned area with a minimum in the middle of 8 nA (~ 20 %) maximum deviation from the linear trend correlated with a deformation of the entrance window due to pressure difference;
3. A periodic structure (see blueish vertical lines) of step 1 cm, with a pronounced decrease in current of 14 nA (~40 %) correlated with the cell structure of the honeycomb (HC) used in the reinforcement of the entrance window;
4. A periodic structure (see reddish vertical lines) of step 3 mm, with an increase in current of 4 nA (~5 %) wrt. the neighboring regions, correlated with the position of anode wires;
5. A non-periodic structure which show regions of HC cells higher than the general trend, correlated with cells for which there is an infiltration of $ArCO_2$

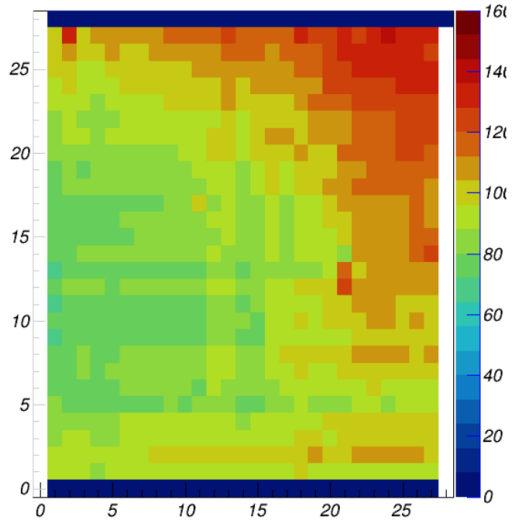

Fig. 6: Anode current measured on the surface of the TRD2D detector after correction for gas leaks and HC cell structure

from the active volume due to microscopic defects on the structure of the drift electrode (~ 15 -20 %);

6. One anode wire with clear connection problems at position ~ 445 mm.

In Fig. 6, a 2D scan of the whole area was performed, with a step of 2 cm such as to avoid the HC cell structure and correct for the gas leaks through the drift electrode. The surface show a pillow like shape characteristic for the mechanical deformation of the entrance window under pressure difference.

The results presented above describe different tests performed on components, procedures or/and the final product in order to asses the quality of the chamber before being send for installation in the CBM setup. The X ray (6 keV) absorption measurements suggest an entrance window with a non negligible massive structure (HC cell walls) and an insufficient rigidity wrt. gas pressure difference. The main problem was the detection of leaks in the drift electrode which lead to migration of gas from the active area to the entrance widow, effectively increasing the absorption for soft X rays outside the active volume. Additionally the measurements show some problems in assuring the parallelism of some of the chamber's components during construction.

2.3 CBM-TRD – 2D Front-end electronics

During the last year, a new “flip-chip” packaging for FASP was developed and tested. Although initial tests were successful, an unexpected issue showed up during the assembly of the packaged chip on the FASPRO3-F2 front-end board. On many assembled chips the channel 0 presented abnormal voltage. Also, on some chips, half of the chip was not functioning. This issues showed up only after the chips were soldered on the board, tests before this stage passed. Also, this issue was not observed in the previous packaging variants. The issue was investigated and found compatible with the hypothesis that fractures are happening on the vias present on the flip-chip substrate during the reflow process.

As flip-chip packaging also showed a low yield, we decided to develop a new package, one which would avoid the reflow process. A solution to package FASP on the flat cable from the pad-plane to the front-end board is currently under development.

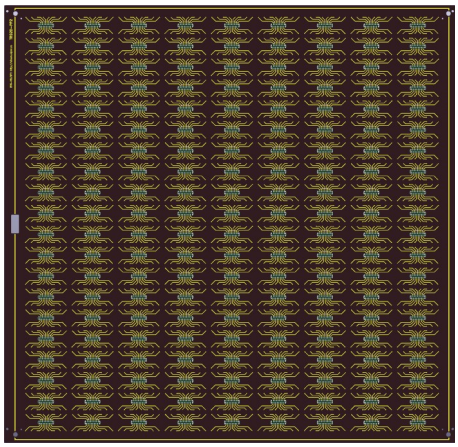

Fig.1e The new design should also improve the manufacturability of the pad-plane.

In order to facilitate this new package solution, it was necessary to modify the design of the pad-plane in order to accommodate connectors for the flat cable. The new design is presented in the figure Fig.1e.

In this circumstance, the development of an advanced testing board, specific to the flip-chip packaging, was delayed until the design of the new packaging is complete

- Describe the progress in achieving the project goals
  The design of the CBM-TOF inner wall is based on the direct flow prototypes. All three type granularity prototypes will be assembled and implemented in the CBM-TOF inner wall modules. The assembling of the first CBM-TOF inner wall module M0 is work in progress.

3. Deliverables

- Scientific reports

List of CBM Progress Reports:

1. V. Aprodu et al., "Status of the construction of the first module (M0) of the CBM-TOF inner wall", CBM Progress Report 2023 (2024), 112; DOII: 10.15120/GSI-2024-00765

2. M. Petris et al., "Aging studies of direct flow MSMGRPC based on fishing line spacers", CBM Progress Report 2023 (2024), 114; DOII: 10.15120/GSI-2024-00765

3. M. Petris et al., "Aging studies of direct flow MSMGRPC based on discrete spacers", CBM Progress Report 2023 (2024), 116; DOII: 10.15120/GSI-2024-00765

V. Aprodu , A. Bercuci , G. Caragheorgheopol , V. Cătănescu , A. Herghelegiu , A. Naziru ,

M. Petriş, M. Petrovici, A. Radu, L. Radulescu , C. Şchiaua , and G. Stoian; *Steps towards TRD2D assembly and tests*, CBM Progress Report 2023, ISBN 978-3-9822127-2-2, p101;

A. Bercuci, E. Clerkin , and A. Puntke; *A more flexible and reliable description of the TRD setup,* CBM Progress Report 2023, ISBN 978-3-9822127-2-2, p106;

C. Şchiaua, A. Bercuci, G. Caragheorgheopol, and V. Cătănescu, *The TRD2D Front-End Board (FEB) for CBM*, CBM Progress Report 2023, ISBN 978-3-9822127-2-2 , p 107;

A. Bercuci, S. Gorbunov, N. Herrmann , and C. Sturm; *Investigations of event vertex reconstruction in mCBM as application of CA tracking and alignment*, CBM Progress Report 2023, ISBN 978-3-9822127-2-2 , p217;

- List of papers (preprints, journal, conference proceedings)
  1. M. Petriş, V. Aprodu, D.Bartoş, D. Dorobanţu, V. Duţă, M. Petrovici, A. Radu, "Aging suppression in Multistrip Multigap Resistive Plate Chambers for high counting rate

experiments", Nuclear Inst. and Methods in Physics Research A, 1066 (2024) 169584 https://doi.org/10.1016/j.nima.2024.169584

- List of talks of the group members (title, conference, date)
  List of Conferences.

  1. M. Petriş et al., "Radiation hard Multi-Strip Multi-Gap Resistive Plate Chamber architecture for low polar angles of the CBM-TOF wall", XVII Workshop on Resistive Plate Chambers and Related Detectors, Santiago de Compostela, Spain, 09 – 13 September 2024

List of presentations at the CBM Collaboration Meetings:

1. M. Petris et al., "Status and plans for the CBM-TOF inner wall", 43rd CBM Collaboration Meeting, GSI Darmstadt, 4 – 8 March 2024
2. M. Petris et al., "CBM-TOF inner wall status and plans", 44th CBM Collaboration Meeting, Prague, 15 – 20 September 2024

A. Bercuci et al., *Status of TRD2D construction and tests,*

43th CBM CM, GSI Darmstadt, 4-8 March 2024

https://indico.gsi.de/event/19018/contributions/78530/attachments/46755/66772/Trd2d-status.pdf

A. Bercuci et al., *Status of TRDs performance as derived from mCBM 22 data*

43th CBM CM, GSI Darmstadt, 4-8 March 2024

https://indico.gsi.de/event/19018/contributions/78531/attachments/46707/66775/Trd-performance.pdf

A. Bercuci et al., *Applying the CBM reconstruction package to mCBM data 2022*

43th CBM CM, GSI Darmstadt, 4-8 March 2024

https://indico.gsi.de/event/19018/contributions/78502/attachments/46838/66909/mCbm-CA.pdf

A. Bercuci et al., *Plans for the TRD2D upgrade*

43th CBM CM, GSI Darmstadt, 4-8 March 2024

https://indico.gsi.de/event/19018/contributions/78510/attachments/46760/66779/Trd2d-mCBM24.pdf

A. Bercuci et al., *TRD2D production status; the chamber and the associated FEE*

44th CBM CM, Czech Technical University in Prague, 15-20 September 2024;

https://indico.gsi.de/event/19534/contributions/82384/attachments/48597/70504/Trd2d_AB_240916.pdf

A. Bercuci et al., *A QA framework for a uniform view on CBM measurements and MC. Application to mCBM22/24 data taking campaigns*

44th CBM CM, Czech Technical University in Prague, 15-20 September 2024;

https://indico.gsi.de/event/19534/contributions/82199/attachments/48667/70662/Qa_AB_240919.pdf

- Other deliverables (TDR, patents, books etc.).

List of student thesis:

1. Daniel Florin Gila, "Studiul comportarii detectorilor MSMGRPC operati in regim de curgere directa a gazului de operare si distantiere discrete la doze mari de iradiere".

C. Şchiaua, A. Bercuci, M. Petrovici

Conceptual Design Report (CDR) TRD2D FEB 18.11.2024,
https://indico.gsi.de/event/20885/

4. Further group activities (max 1 page)

- Collaborations, local synergies, education, outreach
  1. web-site: niham.nipne.ro
  2. Exhibition at National Museum of Geology:" Discover the Universe: Quanta journey to the beginnings", 03 – 30 October 2024
  3. DFH Currier no.6, no.7 (2024).
  4. MSMGRPC and TRD-2D assembling movies.

5. Research plan and goals for the next year (max 1 page)

The design of the inner zone of CBM ToF based on the new architecture of MSMGRPC, fulfilling the granularity and counting rate requirements as a function of polar angles, will be updated. Extensive tests of the performance of the direct flow MSMGRPCs equipped with the readout electronic chain designed and built for the inner zone of the CBM-ToF wall, in real operation condition, în the mCBM setup will be performed.

A re-design of this component was decided in order to address the observations and several recommendations were generated for the assembly steps. A new prototype will be realized to test currently proposed solutions.

The performances of the TRD2D wrt. the position and energy resolution can be studied if a reference measurement, with better performances, is considered. The combination of all tracking detectors at mCBM can offer such a reference by combined analysis via common calibration and alignment. A correlated analysis of mCBM TRD-2D data with TRD-1D, STS and ToF detectors will be performed for an unbiased characterization of the position and energy resolution.